High-Pressure Mechanistic, Bioinorganic NO Chemistry

Subjects: Chemistry, Applied

Contributor: Rudi van Eldik, Maria Oszajca, Justyna Polaczek, Dominika Porębska, Łukasz Orzeł

Nitric oxide (NO) is a short-living free radical, and, in contrast to many signaling agents (e.g., various peptides), which rely on receptors where structural relationships determine their function, the chemistry of NO determines its biological roles. There are two distinct reaction types—direct and indirect—which depend on the NO concentration, reactive species formed and reaction kinetics. The direct effects involve interactions of NO itself with biological targets such as redox metal centers, redox-active amino acids, or other radical species.

Keywords: kinetics ; high-pressure techniques ; nitric oxide ; iron complexes ; porphyrins ; heme proteins ; cobalamins

1. Introduction

Pressure as an experimental variable can provide unique information about the microscopic properties of the studied materials and processes. It can be used as a research tool for investigating the structure, energetics, dynamics, and kinetics of various processes and reactions at the molecular level, as well as to chemical synthesis and modifications of materials to preserve or improve their quality. High-pressure kinetic and thermodynamic studies for the elucidation of reaction mechanisms are usually limited to 200 MPa [1][2][3].

From the temperature dependence of rate constants and application of the transition state theory, the determination of the enthalpy of activation ($\Delta H^{\ddagger}$) and the entropy of activation ($\Delta S^{\ddagger}$)—parameters required for the reaction free energy profile is possible. The additional application of high-pressure kinetic techniques can reveal crucial mechanistic information for chemical processes through the construction of volume profiles with experimentally determined volumes of activation ($\Delta V^{\ddagger}$) (see Chart 1 (A) and (B)). Activation volumes are determined from the slope of plots of lnk versus pressure as shown in Chart 1 (A)

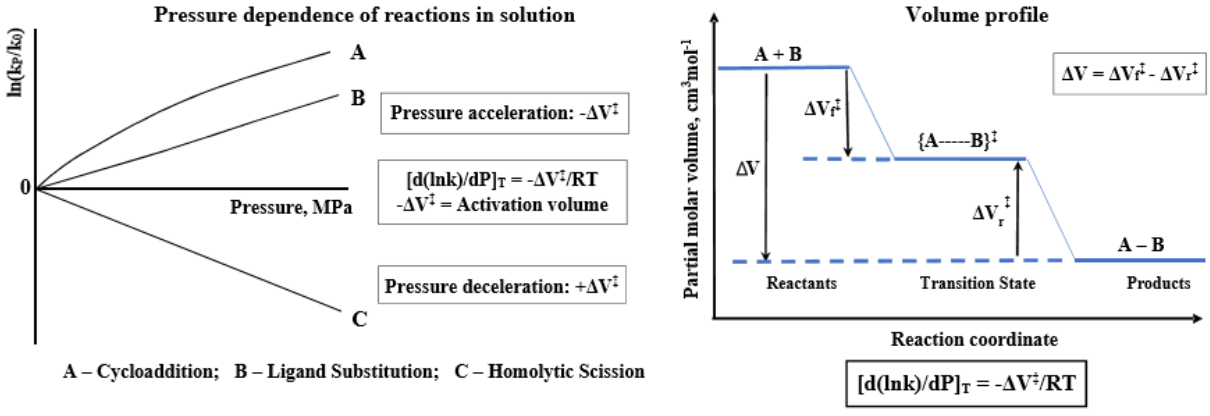

Chart 1. (A) Schematic presentation of the dependence of $\ln(k_p/k_0)$ vs. pressure. **(B)** Schematic presentation of a typical volume profile.

2. High-Pressure Kinetic Techniques Applied to Mechanistic Studies in Coordination Chemistry

The techniques include stopped-flow, flash-photolysis, pulse-radiolysis, T-jump, and NMR high-pressure developments in the pressure range up to 200 MPa [4][5][6][7][8][9][10][11][12]. A typical high-pressure cell is shown in Figure 1.

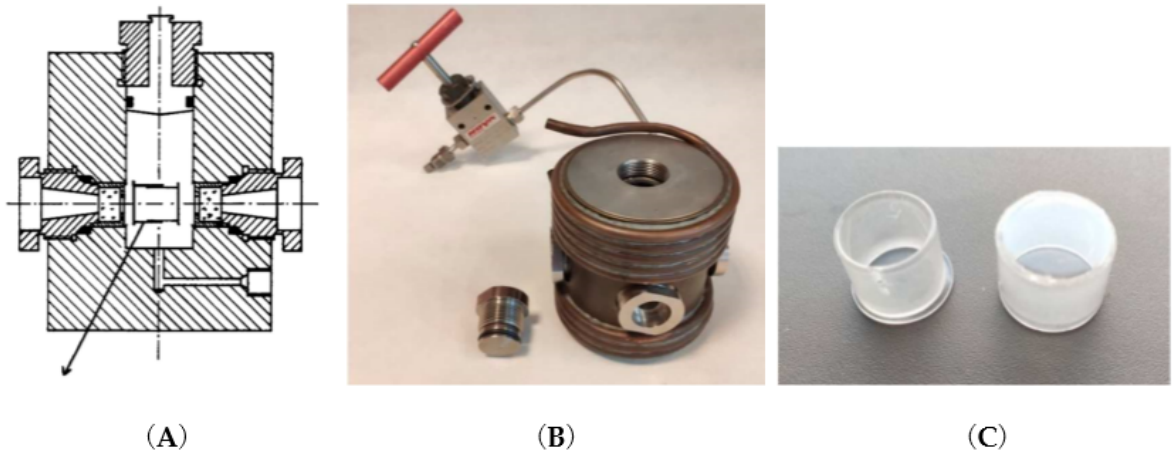

Figure 1. (**A**) Two-window optical high-pressure cell consisting of 1 cm–thick quartz windows and sealed by O- and Δ-rings for pressures up to 200 MPa. Usually the pressure medium is water and is thermostated by an outer copper coil shown in (**B**). The pill-box consists of two closely fitting quartz cylinders which allow compression of the solution inside the cell. There is a special hole drilled through both cylinders by which the pill-box optical cell can be filled and sealed by turning the two cylinders 180° apart. (**B**) Four-window optical high-pressure cell with a thermostating copper coil. (**C**) Two separated cylinders of the pill-box optical cell that make a gastight fit.

An advanced technical development involved the construction of a stopped-flow system within a high pressure cell for experiments up to 200 MPa [6] (see Figure 2).

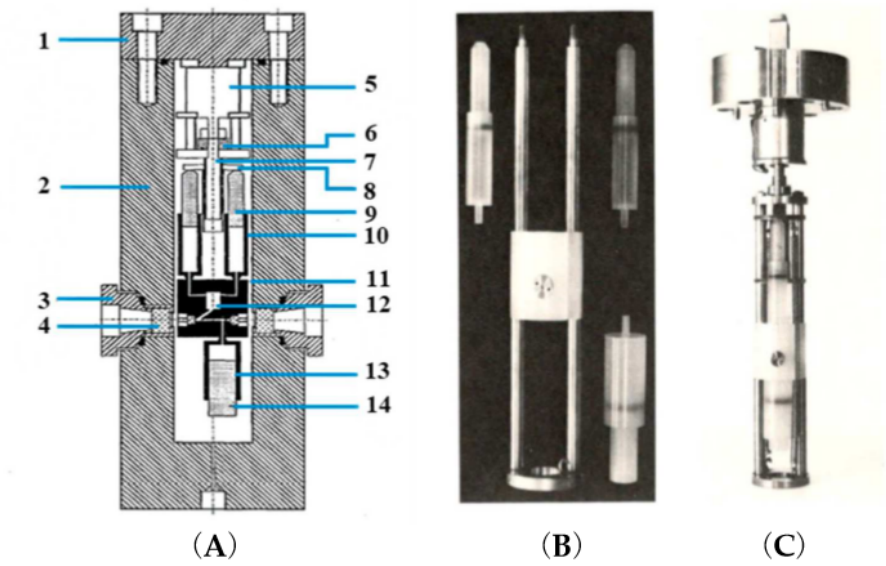

Figure 2. (**A**) Cross-sectional diagram of the high-pressure vessel and stopped-flow apparatus. (1) Pressure vessel lid, (2) pressure vessel, (3) high-pressure window seal assembly, (4) high-pressure sapphire window, (5) step motor, (6) screwdrive mechanism, (7) drive shaft, (8) syringe thrust plate, (9) reactant syringe pistons, (10) reactant syringes, (11) Kel-F cell block, (12) mixing jet, (13) receiver syringe, and (14) receiver-syringe piston. (**B**) High-pressure stopped-flow instrument as constructed by van Eldik and co-workers [6]. Essential components, such as syringes and mixing chamber. (**C**) Complete unit attached to the lid of the high pressure cell.

Finally, we constructed a high pressure NMR probe-head to fit into a narrow bore magnet (see Figure 3), which in the meantime has been commercialized by the Bruker NMR Co.

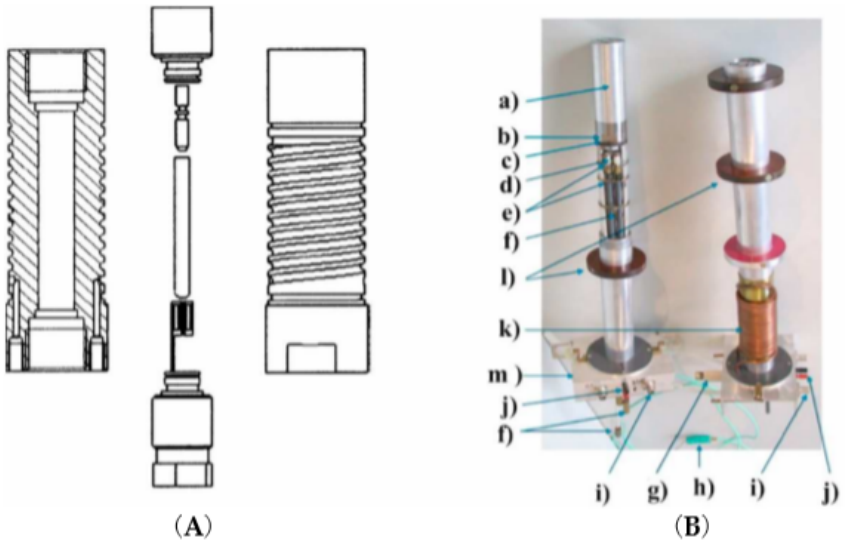

Figure 3. (**A**) Cross-sectional view of the high-pressure autoclave with top and bottom plug, sample tube, macor plug and sample coil. (**B**) Photograph of two narrow bore probe heads: (a) aluminum jacket sealing the double helix used for thermostating, (b) high-pressure vessel, (c) platform carrying the autoclave, (d) capacitors, (e) capacitor platforms, (f) tuning rods, (g) high-pressure connector, (h) thermocouple, (i) BNC connector, (j) Pt-100 connector, (k) copper tubing, and (l) wide-bore adapter [10].

3. NO Binding to Heme Proteins and Model Iron Porphyrin Complexes

Volume profiles that clearly visualize the position of the transition state can be constructed based on the obtained activation volumes. Examples of volume profiles constructed for the ferric TMPS porphyrin are presented in Figure 4 as a function of pH. Due to the six-coordinate nature of ferri–heme complexes, the large positive $\Delta V^{\ddagger}_{on}$ values provided support for a dissociatively activated mechanism with the limiting step being the dissociation of a water molecule. In contrast, for pentacoordinate ferricmonohydroxo TMPS much slower reaction rates, concomitant with negative $\Delta V^{\ddagger}_{on}$ allowed to conclude that the reactivity pattern is not always controlled by the lability of the iron(III) center, but can be also governed by the spin density reorganization and accompanying structural changes. Comparison of typical volume profiles determined for six-coordinate diaqua vs. five-coordinate monohydroxo iron(III) porphyrins are presented in Figure 4.

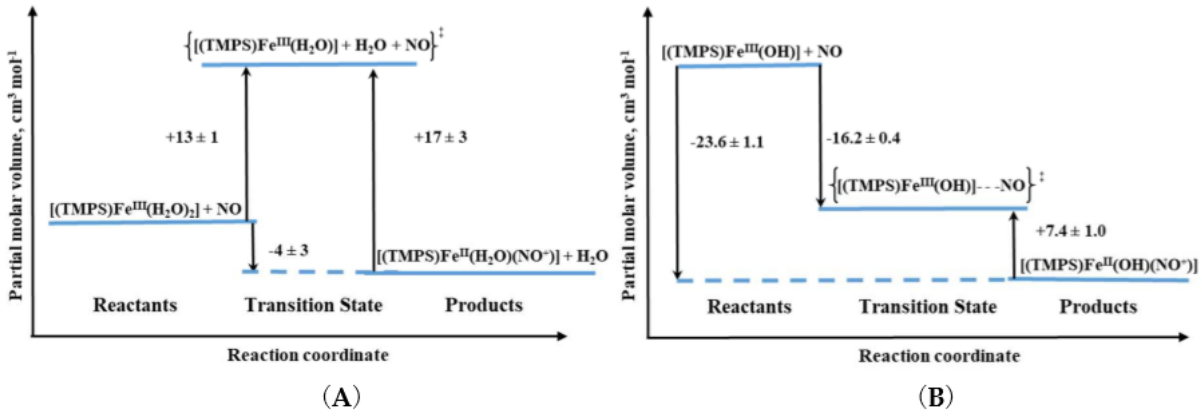

Figure 4. Volume profiles for reversible NO binding to Fe(TMPS) (**A**) $(TMPS)Fe^{III}(H_2O)_2$ and (**B**) $(TMPS)Fe^{III}(OH)$ under acidic and alkaline conditions, respectively [13][14].

High-pressure studies on the nitrosylation of two P450 forms: six-coordinate substrate free and five-coordinate substrate bound, revealed different nitrosylation mechanisms [15]. For substrate-free cytochrome P450 positive values of $\Delta V^{\ddagger}_{on}$ and $\Delta S^{\ddagger}_{on}$ were determined. The positive $\Delta V^{\ddagger}_{on}$ corresponds to a typical limiting dissociative ligand-substitution mechanism, in which the dissociation of coordinated water limits the NO binding rate. Large $\Delta V^{\ddagger}_{on}$ = +28 cm^3/mol represents a relatively higher structural rearrangement in the protein pocket of the substrate-free P450, as well as a spin-state change on going from the low-spin six-coordinate complex to high-spin five-coordinate transition-state intermediate [15] (see Figure 5A). The much smaller positive $\Delta V^{\ddagger}_{on}$ = 6 cm^3/mol was determined for NO binding to synthetic heme–thiolate six-coordinate complex (SR) in methanol [16], a model of P450 cytochrome, allowing us to estimate the participation of factors other than Fe^{III}-H_2O bond breakage (spin-state change and reorganization in the protein pocket). For P450(camph), a completely

different mechanistic pathway was observed that is expressed by negative values for both activation volume and entropy determined for NO binding. Substantially negative $\Delta V^{\ddagger}_{on}$ is consistent with the five-coordinate nature of P450(camph) form, for which the formation of an [(Por)Fe^{III}||(NO)] intermediate complex before NO binding is expected [15] (see Figure 5B).

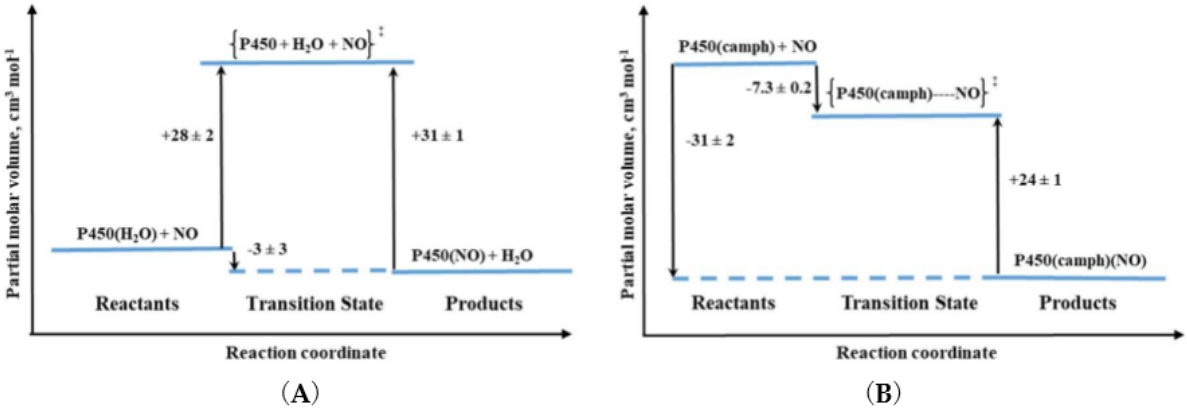

Figure 5. Volume profiles for reversible NO binding to (**A**) substrate-free (P450) and (**B**) camphor bound (P450(camph)) cytochrome.

4. Reactions of NO with Model Fe^{II} Complexes

An interesting example of the application of high-pressure methods to improve our understanding of the underlying mechanism is the reaction known to every high school chemistry student, the so-called “brown-ring test” for nitrate [17]. The process involves the formation of a characteristic green-brown colored ring at the junction of the two solutions layers. This brown-green color is provided by the formation of a Fe-NO complex in the reaction between $[Fe(H_2O)_6]^{2+}$ and NO. During the reaction, one water molecule in $[Fe(H_2O)_6]^{2+}$ is displaced rapidly by the NO molecule (k_{on} = 1.42 × 10^6 M^{-1} s^{-1}). Detailed studies [17] showed that the product is formally stabilized as the Fe^{III}-NO^- complex in which electron density is shifted from the metal center to the NO ligand. The back reaction involves the formation of $[Fe(H_2O)_6]^{2+}$ and release of NO (k_{off} = 3240 ± 750 s^{-1}). The effect of pressure on the described reaction was studied using the high-pressure flash-photolysis technique in the pressure range 0.1–170 MPa (20 °C, pH = 5.0, 0.2 M acetate buffer) resulting in small positive volumes of activation: +6.1 ± 0.2 cm^3 mol^{-1} and +1.3 ± 0.2 cm^3 mol^{-1} for the “on” and “off” reactions, respectively. The activation parameters obtained from the applied measurements suggest that in both processes ligand substitution follows a dissociative interchange (I_d) process [17]. Thus, it can be concluded that the forward reaction involves partial Fe-H_2O bond breakage, prior to NO binding, whereas in the back reaction the Fe-NO bond partially dissociates and is followed by the coordination of H_2O. This is shown in the volume profile for the reaction presented in Figure 6.

Mechanistic studies on the water-exchange reaction in $[Fe(H_2O)_6]^{2+}$ were performed using high pressure NMR techniques (HP ^{17}O-NMR) as described in Section 2 of this review. The water-exchange reaction has a rate constant of 4.4 × 10^6 s^{-1} at 20 °C and the volume of activation for this reaction was reported to be +3.8 ± 0.2 cm^3 mol^{-1}, which suggests that it also follows a dissociative interchange (I_d) mechanism [18]. This means that both the nitrosylation and water-exchange reactions for $[Fe(H_2O)_6]^{2+}$ occur according to the same I_d mechanism for which the water exchange process controls both the rate and the nature of the NO binding mechanism.

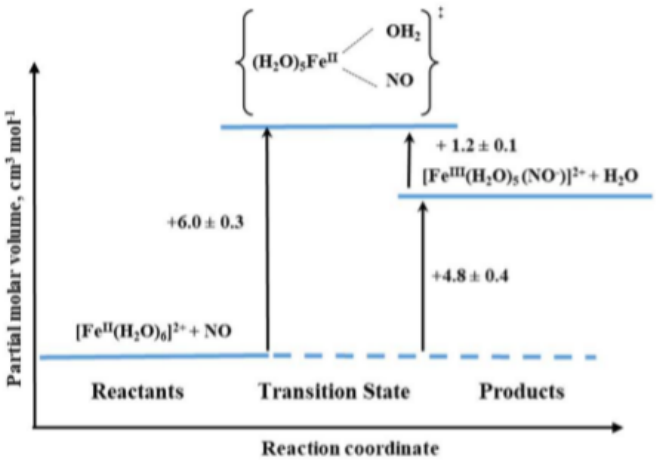

Figure 6. Volume profile for the reaction of $[Fe(H_2O)_6]^{2+}$ with NO.

The other iron(II) complexes, for which reactions with nitric oxide have been studied with the application of high pressure methods, were polyaminecarboxylate complexes. With the only one exception for all studied complexes, small positive activation volumes obtained, suggested an I_d mechanism. Thus, the most probable sequence during the reaction is again the partial Fe-H_2O bond breakage, followed by NO binding as was also described above for the $[Fe(H_2O)_6]^{2+}$ complex [19]. Only in the case of the nitrilotriacetate (nta) complex, negative activation volume was found, indicating an associative interchange (I_a) mechanism for the nitrosylation reaction and suggesting that the reaction involves partial Fe-NO bond formation prior to the release of H_2O. This perfectly agrees with the six-coordinate nature of the nta complex compared to the seven-coordinate nature of the $[Fe^{II}(edta)(H_2O)]^{2+}$ complex as shown in Figure 7.

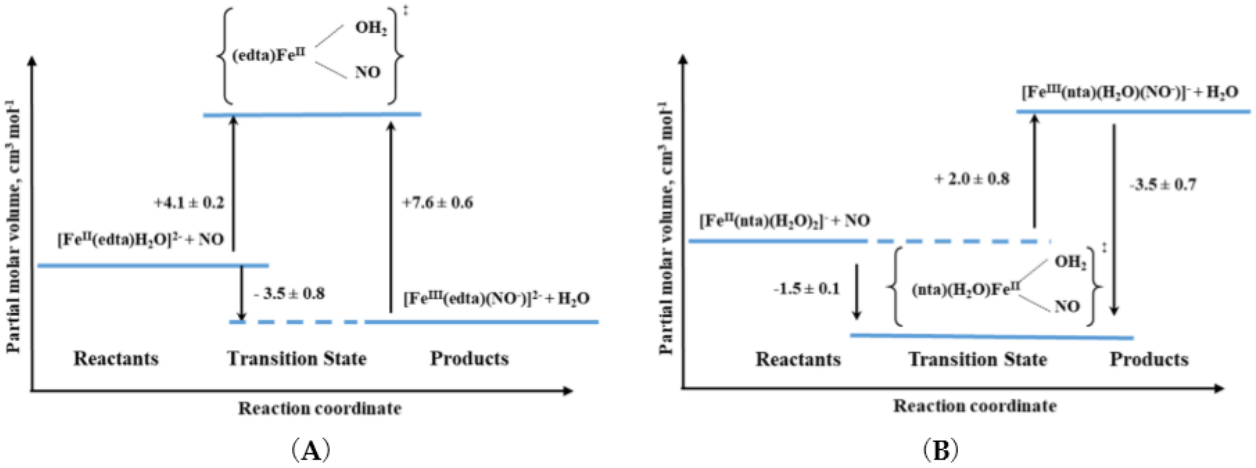

Figure 7. Volume profiles for the reactions of (**A**) seven-coordinate $[Fe^{II}(edta)(H_2O)]^{2+}$ and (**B**) six-coordinate $[Fe^{II}(nta)(H_2O)_2]^{2+}$ complexes with NO [19].

5. NO Binding to Cobalamin and Cobalt Porphyrins

While the issue of the potential interaction of Cbl(H_2O) with NO has remained controversial for many years, such a reaction with Cbl(II) is virtually indisputable. It is supported by unequivocal evidence provided by a variety of spectroscopic techniques (UV–Vis, ^{1}H-, ^{15}N-, and ^{31}P NMR). The results of kinetic investigations indicate a very high equilibrium constant (10^8 M^{-1} at pH = 7.0) for the following reaction:

Cbl(II) + NO ↔ Cbl(NO)

Based on NMR studies, the actual form of the final product was defined as Cbl(III)(NO^-), in agreement with the products of reductive nitrosylation of Cbl(H_2O) and Co(III) porphyrins. The activation parameters were determined for both the formation and decay of the nitrosyl complex by using laser flash photolysis and stopped-flow techniques, respectively. The effect of pressure was studied for both reactions. The small positive value of $\Delta V^{\ddagger}_{on}$ for Cbl(III)(NO^-) formation (+5.4 cm^3/mol at pH = 7.4) suggested implementation of the dissociative interchange mechanism, which was possible due to the appearance of a water-bound intermediate. A similar type of mechanism is being realized in the reverse reaction forced by the use of NO-trapping technique, as indicated by the value of $\Delta V^{\ddagger}_{off}$ = +7.9 cm^3/mol. The volume profile for the reaction is shown in Figure 8.

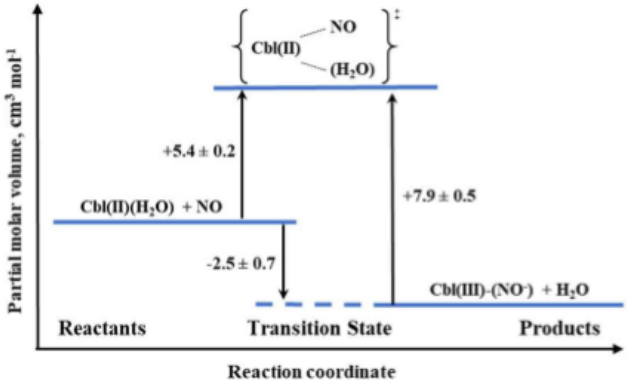

Figure 8. The volume profile for the reaction of Cbl(II) with NO in aqueous solution at pH = 7.4.

6. Conclusions

High-pressure techniques for kinetic and mechanistic studies represent a unique and irreplaceable tool in the elucidation of reaction mechanisms in solution. The information provided by the activation volume makes it possible to unambiguously determine the nature of the underlying reaction mechanism, which gives an advantage over the activation entropy obtained by analyzing the effect of temperature. Despite the technical complexity, due in part to the relatively slow establishment of equilibrium in solution after a change in applied hydrostatic pressure, it is possible to follow the course of reactions occurring over a wide range of timescales by combining the high-pressure technique with standard, stopped-flow, and relaxation (laser flash photolysis and pulse radiolysis) techniques. This is particularly useful for studying fast inorganic reactions, which, in solution, are often applicable to biological and catalytic systems.

References

1. Holzapfel, W.; Isaacs, N.. High Pressure Techniques in Chemistry and Physics: A Practical Approach; Oxford University Press: Oxford, 1997; pp. p.388.
2. van Eldik, R.. Inorganic High Pressure Chemistry: Kinetics and Mechanisms; Elsevier: Amsterdam, 1986; pp. p.448.
3. Winter, R.; Jonas, J.. High Pressure Molecular Science; Springer: Dordrecht, 1999; pp. vol. 358, p. 559.
4. Doss, R.; van Eldik, R.; Kelm, H.; Construction and testing of a high-pressure joule-heating temperature-jump apparatus.. *Rev. Sci. Instrum.* **1982**, *53*, 1592-1595, .
5. Spitzer, M.; Gartig, F.; van Eldik, R.; Compact, transportable, and multipurpose high-pressure unit for UV–VIS spectroscopic measurements at pressures up to 200 MPa.. *Rev. Sci. Instrum.* **1988**, *59*, 2092-2093, .
6. van Eldik, R.; Gaede, W.; Wieland, S.; Kraft, J.; Spitzer, M.; Palmer, D.A.; Spectrophotometric stopped-flow apparatus suitable for high pressure experiments to 200 MPa.. *Rev. Sci. Instrum.* **1993**, *64*, 1355-1357, .
7. Wieland, S.; van Eldik, R.; Apparatus for filling the pillbox high-pressure optical cell under unaerobic conditions.. *Rev. Sci. Instrum.* **1989**, *60*, 955-956, .
8. Wishart, J.F.; van Eldik, R.; High-pressure pulse radiolysis. Modification of an optical cell for 2-MeV electron pulse radiolysis at pressures up to 200 MPa.. *Rev. Sci. Instrum.* **1992**, *63*, 3224-3225, .
9. Zahl, A.; Igel, P.; Weller, M.; Koshtariya, D.; Hamza, M.S.A.; van Eldik, R.; Compact high pressure unit for ultraviolet-visible-near-infrared spectroscopic measurements at pressures up to 400 MPa.. *Rev. Sci. Instrum.* **2003**, *74*, 3758-3762, .
10. Zahl, A.; Igel, P.; Weller, M.; van Eldik, R.; High-pressure nuclear magnetic resonance probe designed for a narrow bore magnet system.. *Rev. Sci. Instrum.* **2004**, *75*, 3152-3157, .
11. Zahl, A.; Neubrand, A.; Aygen, S.; van Eldik, R.; A high-pressure NMR probehead for measurements at 400 MHz.. *Rev. Sci. Instrum.* **1994**, *65*, 882-886, .
12. Wanat, A.; Wolak, M.; Orzeł, Ł.; Brindell, M.; van Eldik, R.; Stochel, G.; Laser flash photolysis as tool in the elucidation of the nitric oxide binding mechanism to metallobiomolecules.. *Coord. Chem. Rev.* **2002**, *229*, 37-49, .
13. Laverman, L.E.; Ford, P.C.; Mechanistic Studies of Nitric Oxide Reactions with Water Soluble Iron(II), Cobalt(II), and Iron(III) Porphyrin Complexes in Aqueous Solutions: Implications for Biological Activity. *J. Am. Chem. Soc.* **2001**, *123*, 11614-11622, .
14. Wolak, M.; van Eldik, R.; pH controls the rate andmechanism of nitrosylation of water-soluble FeIII porphyrin complexes.. *J. Am. Chem. Soc.* **2005**, *127*, 13312-13315, .
15. Franke, A.; Stochel, G.; Jung, C.; van Eldik, R.; Substrate binding favors enhanced NO binding to P450(cam).. *J. Am. Chem. Soc.* **2004**, *126*, 4181-4191, .
16. Franke, A.; Stochel, G.; Suzuki, N.; Higuchi, T.; Okuzono, K.; van Eldik, R.; Mechanistic studies on the binding of nitric oxide to a synthetic heme-thiolate complex relevant to cytochrome P450.. *J. Am. Chem. Soc.* **2005**, *127*, 5360-5375, .
17. Wanat, A.; Schneppensieper, T.; Stochel, G.; van Eldik, R.; Bill, E.; Wieghardt, K.; Kinetics, mechanism, and spectroscopy of the reversible binding of nitric oxide to aquated iron(II). An undergraduate text book reaction revisited.. *Inorg. Chem.* **2002**, *41*, 4-10, .
18. Maigut, J.; Meier, R.; Zahl, A.; van Eldik, R.; Elucidation of the solution structure and water-exchange mechanism of paramagnetic [FeII(edta)(H2O)]2-.. *Inorg. Chem.* **2007**, *46*, 5361-5371, .

19. Schneppensieper, T.; Wanat, A.; Stochel, G.; van Eldik, R.; Mechanistic information on the reversible binding of NO to selected iron(II) chelates from activation parameters.. *Inorg. Chem.* **2002**, *41*, 2565-2573, .